Available online at www.sciencedirect.com
SCIENCE DIRECT®
Journal of Chromatography A, 1077 (2005) 143–150
JOURNAL OF CHROMATOGRAPHY A
www.elsevier.com/locate/chroma

Variations of particle size and bed voidage distributions in expanded bed during transient operation processes

Zheng Yang, Yan Sun *

Department of Biochemical Engineering, School of Chemical Engineering and Technology, Tianjin University, Tianjin 300072, China

Received 20 April 2004; received in revised form 3 January 2005; accepted 25 April 2005

Abstract

Changes in bed expansion are frequently encountered during an expanded bed adsorption, such as during the initial bed expansion, feed loading and washing processes. We have here studied the changes of local particle size distribution and bed voidage of an expanded bed in the initial bed expansion process as well as those during the changes in mobile phase viscosity, which imitated feed loading and column washing processes. Using a glass column modified with three side sampling ports and Streamline AC as the solid phase, experimental measurements on a series of operation moments during the transient processes were carried out by sampling the particles from within the column at different axial positions. In the initial bed expansion process, the gradual formation of an axial classification from a settled bed to a stable expanded bed was first displayed. By changing the mobile phase from water to 10% (w/w) glycerol solution or vice versa, the variations in both the particle size distribution and bed voidage corresponding to the increase or decrease of the bed height caused by the changes of the mobile phase viscosity were examined as well. The transient changes of the local particle size distribution and bed voidage first occurred in the bed bottom and then progressed from bottom to top along the axial direction. However, the changes of bed voidage at different axial positions were not unidirectional. That is, by changing the mobile phase to the high-viscosity glycerol solution, a constant increase of the bed voidage was observed in the bed bottom, while a distinct decrease of the bed voidage before its increase was involved at the middle and top positions. This is ascribed to the compression effect caused by the upward movement of the lower part particles.

Keywords: Expanded bed adsorption; Particle size distribution; Bed voidage; Transient phenomena

1. Introduction

Expanded bed adsorption (EBA) uses a purpose-designed column and adsorbent with a defined size and/or density distribution. In expanded bed operation, an upward flow of mobile phase through the adsorbent bed provides high bed voidage, which makes it possible for the particulate materials to pass through whilst the target bioproduct is adsorbed onto the solid phase. Thus, as a novel integrative technology for downstream bioprocessing, EBA has been widely employed to directly capture target bioproducts from cell containing broth, cell disruptate and other unclarified feedstocks [1–4]. This reduces both the process cost and operation time.

A successful operation of EBA depends on the formation of a stable fluidized bed even in the presence of turbid feedstock, which is characterized by a low back mixing, lack of stagnant zones and an ordered distribution of the adsorbent within the bed. Therefore, a variety of interactions between adsorbent and biomass in feedstock have been investigated to understand the EBA system [5–10]. Moreover, to achieve tighter control of the EBA process and to reach high process efficiency, it is desirable to understand the distribution of particle size and bed voidage within the bed during the operation since the liquid phase dispersion and adsorption behavior in the EBA column have a close relation to the axial particle size distribution [10–13]. Some authors have reported the particle size distributions and bed voidage along the axial height of the bed under stable bed expansion conditions [12,14–16]. However, to date, the information on particle size distribu-

* Corresponding author. Tel.: +86 22 2740 4981; fax: +86 22 2740 6590.
E-mail address: ysun@tju.edu.cn (Y. Sun).

0021-9673/$ – see front matter © 2005 Elsevier B.V. All rights reserved.
doi:10.1016/j.chroma.2005.04.054

tions and bed voidage during transient operation processes is still unavailable.

Generally, the operation of an EBA can be divided into five stages, this is, (1) bed expansion and equilibration with an equilibration buffer, (2) application of feedstock, (3) washing, (4) product elution and (5) cleaning in place. The bed height increases in the bed expansion process. Additionally, the changes of expanded bed height also occur in the other stages due to the changes of mobile phase viscosity and density, if the flow rate is kept unchanged. The transient changes of bed height are especially distinct during the feedstock loading and washing stages, which are the key steps of an EBA process. The first phase of crude and viscous feedstock application leads to the increase of bed height, while bed washing with a low viscosity buffer after the feed loading results in the decrease of bed height. Such variation is particularly important when the feedstock loading volume is small in comparison to the bed volume since the change in bed height will exist during the whole loading process. Therefore, it is paramount to know how the distribution of adsorbent particles and bed voidage change during the transient processes. Such knowledge would help to control the EBA operation and to improve the process modeling and analysis.

In this work, we have studied the changes of local particle size distribution and bed voidage of an expanded bed in the initial bed expansion process as well as those during the changes in mobile phase viscosity, which imitated feed loading and bed washing processes. For this purpose, a glass column modified with side sampling ports was designed to study the transient phenomena. Using the commercial Streamline matrix as the solid phase, experimental measurements of local particle size distribution and bed voidage on different operation moments during the transient processes were carried out by sampling the matrix particles from within the column at different axial positions. As a result, comprehensive information on the transient phenomena in bed expansion, feed loading and washing processes was obtained.

2. Materials and methods

2.1. Solid matrix and chemicals

Streamline quartz base matrix (Streamline AC, Amersham Biosciences, Uppsala, Sweden) was used in all experiments. Its size distribution scanned with a Mastersizer 2000 unit (Malvern Instruments, Malvern, UK) was in the range of 80–500 μm, with a volume-weighted mean diameter of 210 μm. Expanded bed experiments were performed using deionized water and 10% (w/w) glycerol solution as the mobile phases. All other chemicals were of analytical grade from local sources.

2.2. Column design

A homemade glass column (0.7 m height, 25.15 mm I.D.) with a stainless steel mesh (opening size equivalent to 74 μm) as the liquid distributor was used for expanded bed experiments (Fig. 1). Glass beads (0.3–0.4 mm, 2.6 g mL^{-1}) were added in 1 cm height on the bed bottom to improve flow distribution at the column inlet. The glass column design followed that described previously [15], but modified with three sampling ports located at 1.2, 16.2 and 31.2 cm from the surface of the glass beads. Each port was sealed with silicone rubber, and the sealed section was well fit for the smooth inner surface of the column wall. Estimated by the

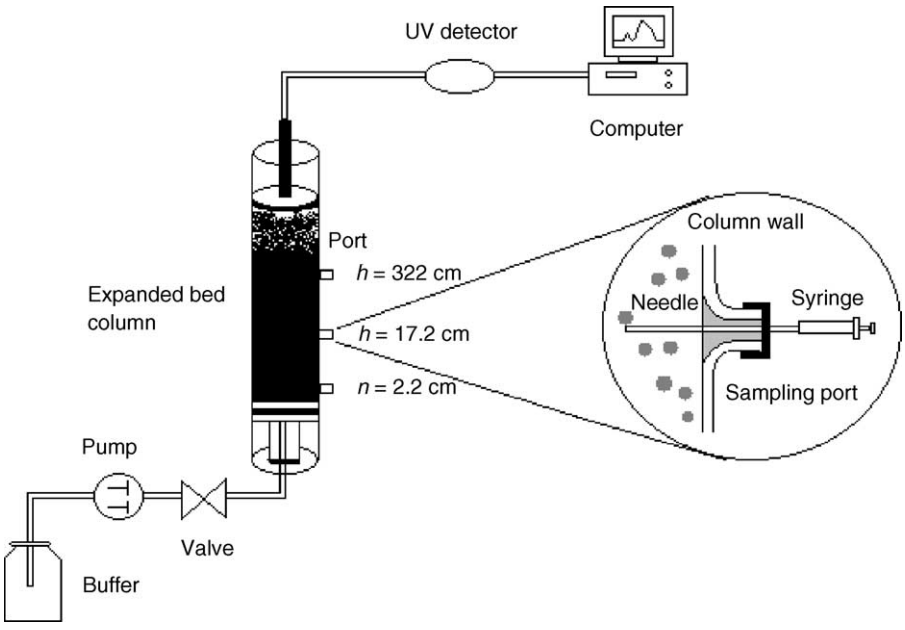

Fig. 1. A schematic diagram of the expanded bed system for sampling.

step-input technique [15,17] with acetone as the tracer, the liquid dispersion level within the modified column was found comparable to that obtained within a STREAMLINE 25 column (1.0 m × 25 mm I.D., Amersham Biosciences) (*Bo* value [15] larger than 40 for a 33 cm expanded bed). A metal needle (90 mm × 2.06 mm O.D., 1.76 mm I.D.) connected to a 2-mL syringe was used to withdraw the liquid–solid suspension samples from within the column. The needle diameter was large enough compared to the particle size so a representative adsorbent sample could be obtained and the selective withdrawal of small particle sizes was avoided. All expanded bed experiments were carried out with ÄKTA Explorer 100 system (Amersham Biosciences, Uppsala, Sweden).

2.3. Experimental design for sampling

All expanded bed experiments were performed with 0.163 m settled bed (81.5 mL Streamline AC). Variations in particle size distribution were measured in three different phases during the expanded bed operation: (I) transient expansion from a settled bed in which the particles were well mixed, to the later stable expanded bed with deionized water; (II) application of 10% (w/w) glycerol solution until a second stable bed expansion, imitating a feed loading process; (III) conversion to deionized water again until a third stable bed expansion, imitating a washing process.

In phase I, the bed was expanded at 5.94×10^{-4} m s^{-1} with deionized water to reach 2.18-fold bed expansion. On a series of prearranged moments during the bed expansion, three needles connected with syringes were inserted into the three sealed ports at different axial heights respectively, and 1.5 mL of liquid–solid suspension sample at each sampling position was withdrawn from the center of the column synchronously. Another bed expansion experiment was done at 8.33×10^{-4} m s^{-1} with a 2.86-fold expansion, and samplings were done on the same sampling moments and positions as that performed at 5.94×10^{-4} m s^{-1}. One sampling procedure took about 3 s. After each sampling, the mobile phase supplying was stopped and the particle size distribution was measured. Before the next bed expansion experiment, all the sampled particles were collected and returned to the column. The settled particles in the bed were well mixed to avoid any pre-classification during the sedimentation process.

In order to investigate the transient behaviors in phases II and III, the bed was typically expanded at 5.94×10^{-4} m s^{-1} for at least 30 min with deionized water. Then, the mobile phase was switched to 10% (w/w) glycerol solution at the same velocity. On some predetermined moments, axial samplings were carried out at the three sampling positions simultaneously. For phase III study, after the bed had been stably expanded with the glycerol solution, deionized water was switched back again and samples were withdrawn from the column center up its axial height in the same way as that during the application of the glycerol solution. The sampling procedures in phases II and III were just as same as those in phase I.

2.4. Particle size distribution and bed voidage measurements

The particle size was measured with a Mastersizer 2000 unit (Malvern Instruments). The particle size distributions were expressed by volumetric diameters d_{10}, d_{50}, and d_{90}. They are defined as the points on the particle distribution where, respectively, 10, 50 and 90% by volume of the particles are smaller than the stated diameter. The d_{10} statistic is therefore an indicator of the proportion of fines in a particle size distribution, while d_{50} shows the mean volume diameter and d_{90} a measure of the proportion of large particles present in the sample. In triplicate experiments, the variations in the values of d_{10}, d_{50} and d_{90} were found within 5%.

The distributions of local bed voidage at different axial heights in phases II and III were estimated with a method based on the removal of the samples from within the bed [16]. The sampling experiments were performed in the same way as those during the measurements of axial particle size distributions on each prearranged moment. About 1.5 mL liquid–solid suspensions were withdrawn from the center of the column, and then the syringes containing samples were placed vertically until all the particles settled steadily (about 1 h). The settled-bed and the total liquid–solid suspension volumes were determined by reading the syringe scales. The local bed voidage φ was then determined by

$$\phi = \frac{\phi_S V_S + V_{LS} - V_S}{V_{LS}} \quad (1)$$

where φ_s is the settled-bed voidage, which was taken to be 0.4 [12,14], V_S is the settled-bed volume, and V_{LS} is the liquid–solid suspension volume.

The sampling work on each position as well as sampling moment was done by triplicate experiments to ensure data reliability, and the results of the particle size and bed voidage were confirmed to be within 5% deviation.

3. Results and discussion

3.1. Transient bed expansion in the three phases and sampling protocol design

The formation of a stable fluidized bed is paramount to a successful EBA operation. The expansion behavior of the particles in the bed is governed by the characteristics of solid matrix, the column design and the mobile phase used in experiment and can be predicted using the classical equations of Stokes and Richardson-Zaki [18]. The Stokes law can be used to predict the terminal velocity, u_t, of an individual particle, assuming plug flow in the column:

$$u_t = \frac{d_p^2 g(\rho_p - \rho)}{18\mu} \quad (2)$$

The effect of fluid velocity, u, on the bed voidage φ can be predicted using the Richardson-Zaki equation:

$$u = u_t \phi^n \quad (3)$$

where n is the Richardson-Zaki exponent.

This work focused on the variations in particle size and voidage distributions during the transient bed expansion processes, so the characteristics of the increase and decrease in bed height during the three phases described above are crucial to the research. In phase I, the Streamline AC, initially settled in the column (81.0 mL), was fluidized in deionized water and the increase of the bed height was recorded continuously at the fluid velocities of 5.94×10^{-4} and 8.33×10^{-4} m s^{-1}, respectively. At 5.94×10^{-4} and 8.33×10^{-4} m s^{-1}, 4.6 and 3.3 min respectively was needed for applying one settled-bed volume (SBV) of mobile phase. In phases II and III, after the Streamline matrix was stably fluidized in deionized water, a 10% (w/w) glycerol solution was applied to the bed, and the transient change in the bed height was recorded. After the bed had reached a new stable expansion, the mobile phase was switched back to deionized water and the decrease of the bed height was recorded as well. Figs. 2 and 3 show the variations in bed height as a function of the mobile phase volume applied under different conditions. Previous publications have stated that approximately six SBV are required to reach a stable expansion in EBA systems [8,19], and the results shown in Figs. 2 and 3 are consistent to their reports.

Based on the results shown in Figs. 2 and 3, we designed the following experimental protocol for sampling at different critical moments: (i) before the change in the bed height (0 SBV for phases II and III); (ii) the very early phase shortly after the switch to a new mobile phase, i.e., 0.65 SBV; (iii) during the transient expansion, i.e., 1.30 SBV; (iv) in the late phase of the transient expansion, i.e., 2.16 SBV; (v) shortly after a new equilibrium was reached, i.e., 6.48 SBV; (vi) long after a stable bed expansion in the mobile phase, i.e., 8.74 SBV.

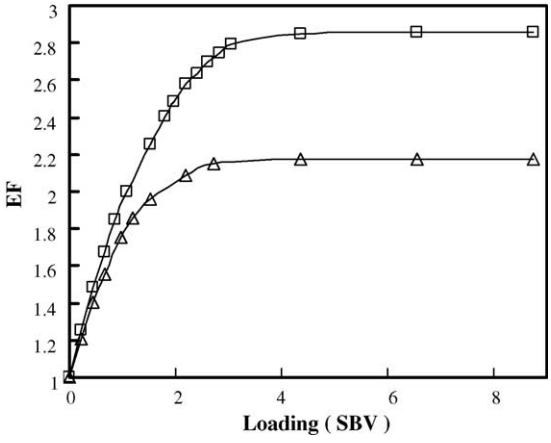

Fig. 2. Transient bed expansion from settled bed to expanded bed in deionized water at liquid flow velocities of (△) 5.94×10^{-4} and (□) 8.33×10^{-4} m s^{-1}. 1 SBV = 4.6 and 3.3 min, respectively, at 5.94×10^{-4} and 8.33×10^{-4} m s^{-1}. EF = H/H_0, H_0 = 16.3 cm (settled bed height).

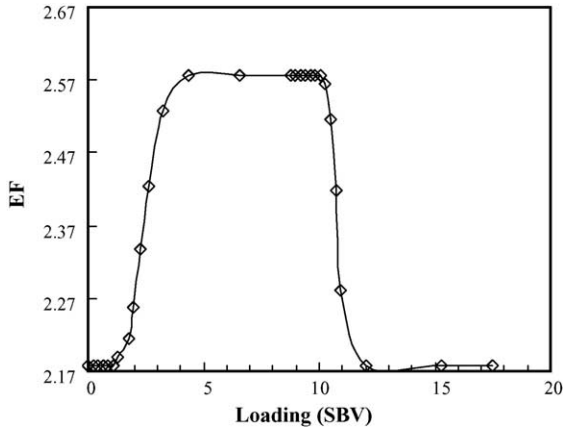

Fig. 3. Transient bed expansion during application of a 10% (w/w) glycerol solution and deionized water to an expanded bed of Streamline AC at 5.94×10^{-4} m s^{-1}. Feed solution was changed from deionized water to glycerol solution at 0 min (0 SBV) and was switched back to the deionized water at 40 min (8.74 SBV). H_0 = 16.3 cm.

3.2. Variations of axial particle size distribution in phase I

Variations in axial particle distribution during transient expansion from settled bed to expanded bed (phase I) at different liquid flow rates were determined at axial heights of 1.2 and 16.2 cm as soon as the loading volume reached 0.65 and 1.30 SBV. In addition, sampling was also performed from the port at 31.2 cm when it reached 2.16 and 6.48 SBV. The results are exhibited in Figs. 4 and 5. It can be seen from the figures that, generally, the Streamline particles in the bed exhibit quite similar trend on each sampling moment during the total process of bed expansion at both the liquid flow rates. The in-bed particles expanded progressively from the well-mixed packed bed to a stably classified fluidized bed. This is the behavior expected in such an expansion process, but this is the first time it has proved possible to confirm this behavior experimentally. The range of particle sizes was larger than that reported by Bruce and Chase [12,20]. It is due to the different particle size distributions employed in this work (80–500 μm, 210 μm on average) and that used by Bruce and Chase (Streamline SP of 100–400 μm, 192 μm on average).

From Figs. 4a and 5a, we can find that shortly after the beginning of the expansion from settled bed to expanded bed (0.65 SBV), the particle size distributions at the two lower positions were quite similar to the bulk Streamline AC. When the loading volume reached 1.30 SBV (Figs. 4b and 5b), small shifts of the particle size distributions at 1.2 and 16.2 cm to higher values were observed, and the increasing extent was more obvious at 8.33×10^{-4} m s^{-1} (Fig. 5b). However, the difference in the particle size distributions between the two heights was still little. The re-

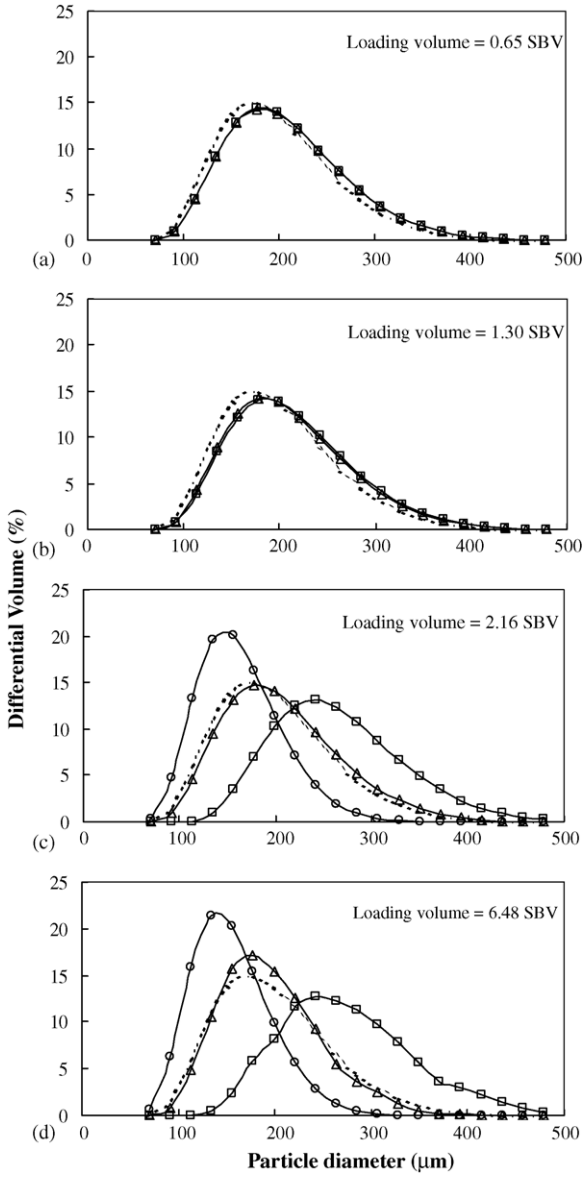

Fig. 4. Variations in particle size distribution during transient expansion from settled bed to expanded bed at axial height of (□) 1.2, (△) 16.2 and (◯) 31.2 cm. Liquid velocity was 5.94×10^{-4} m s^{-1}. The dashed line is the particle size distribution of bulk Streamline AC. H_0 = 16.3 cm.

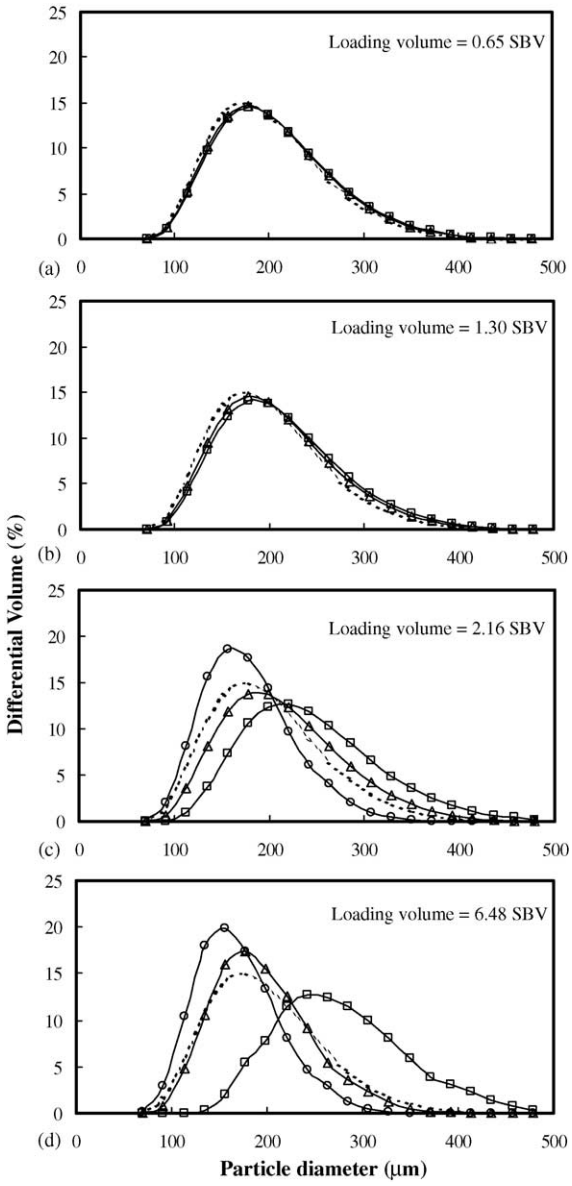

Fig. 5. Variations in particle size distribution during transient expansion from settled bed to expanded bed at axial height of (□) 1.2 cm; (△) 16.2 cm; (◯) 31.2 cm. Liquid velocity was 8.33×10^{-4} m s^{-1}. The dashed line is the particle size distribution of bulk Streamline AC. H_0 = 16.3 cm.

sults indicate that the bed classification had not formed at the moment.

Sampling work at the top port was performed together with that at the lower two positions synchronously when the loading volume of deionized water reached 2.16 SBV. As shown in Figs. 4c and 5c, obvious particle classification was observed at the moment. The mean diameter of the particles from the bottom port became significantly larger than that examined on the last two moments, and the size range decreased a lot. The change in the particle size distribution at 16.2 cm was still insignificant (by comparison of Fig. 4c and Fig. 5c to Fig. 4b and Fig. 5b, respectively) and kept close to the bulk Streamline AC.

The ultimate hydrodynamic bed stability and complete particle classification were reached after 6 SBV of mobile phase loading (Figs. 4d and 5d). The range of particle size distribution at each position became smaller than that shown in Figs. 4c and 5c, respectively. Comparing the results measured at the two different velocities, the mean particle diameter at each sampling height was found slightly larger at 8.33×10^{-4} m s^{-1} than that at 5.94×10^{-4} m s^{-1}. This indicates that the increase of liquid velocity leads to an aggravated particle size classification because of the increased expanded bed height [15]. Mid-sized particles (ca. 200 μm at 5.94×10^{-4} m s^{-1} and ca. 210 μm at 8.33×10^{-4} m s^{-1}) were found in significant quantities at each of the sampling

heights, suggesting the presence of the significant distribution of particles through the column [12].

3.3. Variations in axial particle size and voidage distributions in phases II and III

A 10% (w/w) glycerol solution was employed as feedstock to imitate the feed loading process. Variations in axial particle size distribution and local voidage caused by the changes of the mobile phase density and viscosity were investigated. In Fig. 6, the particle size distribution was expressed by d_{10}, d_{50} and d_{90} as a function of the mobile phase volume.

It can be seen from Fig. 6 that the change of mobile phase had only a small effect on the particle size distribution at the bottom position. That is, the loading of the glycerol solution resulted in a small increase, whereas the recharge of deionized water led to a small decrease of the particle sizes. It is considered due to the larger particle size at the bottom region (volume-weighted mean diameter 292 μm, see Fig. 4d). The larger particles have higher sedimentation velocity, which makes it difficult for them to move upward. Moreover, to keep the bed stable, the bottom layer of the bed should remain the maximum bulk density [21]. In comparison, the particle sizes d_{10}, d_{50} and d_{90} of the samples drawn from 16.2 cm began to increase at a mobile phase volume of 1.30 SBV, and then kept unchanged between 2.16 and 6.48 SBV. At the axial height of 31.2 cm, little change in particle size was observed until the loading volume reached 2.16 SBV, and the transient changes did not stop until a new equilibrium of the expanded bed was achieved (after 6 SBV).

Tong and Sun [15] reported that the effect of liquid viscosity on the axial particle size distribution of Streamline particles was similar to that of liquid velocity because the increases of both the liquid viscosity and flow velocity led to the raise of expanded bed height. Slis et al. [22] stated that following a change in fluidization velocity, the void fraction changed progressively from the distributor upwards, until the bed reached a new steady-state condition. The experimental data obtained here, as shown in Fig. 7, indicate that the changes of bed voidage at different axial positions were not unidirectional. During the application of glycerol solution, the bed voidage at 1.2 cm increased progressively until a new stable situation was reached and decreased in the similar way when the mobile phase was converted back to deionized water. The changes of local voidage at the middle and top positions, however, were quite different during the transient processes. During the initial transient phase, when the loaded glycerol solution was 0.65 SBV, the measurements at the middle position (16.2 cm) showed a decrease in the local voidage. Later, the voidage rebounded when the mobile phase loading reached 1.30 SBV and kept increasing until 6 SBV of the glycerol solution was introduced. When deionized water was challenged to the column again, the local voidage at this position correspondingly increased first and then began to decrease gradually when 1.30 SBV of deionized water (totally 10.04 SBV) was introduced into the system. Then,

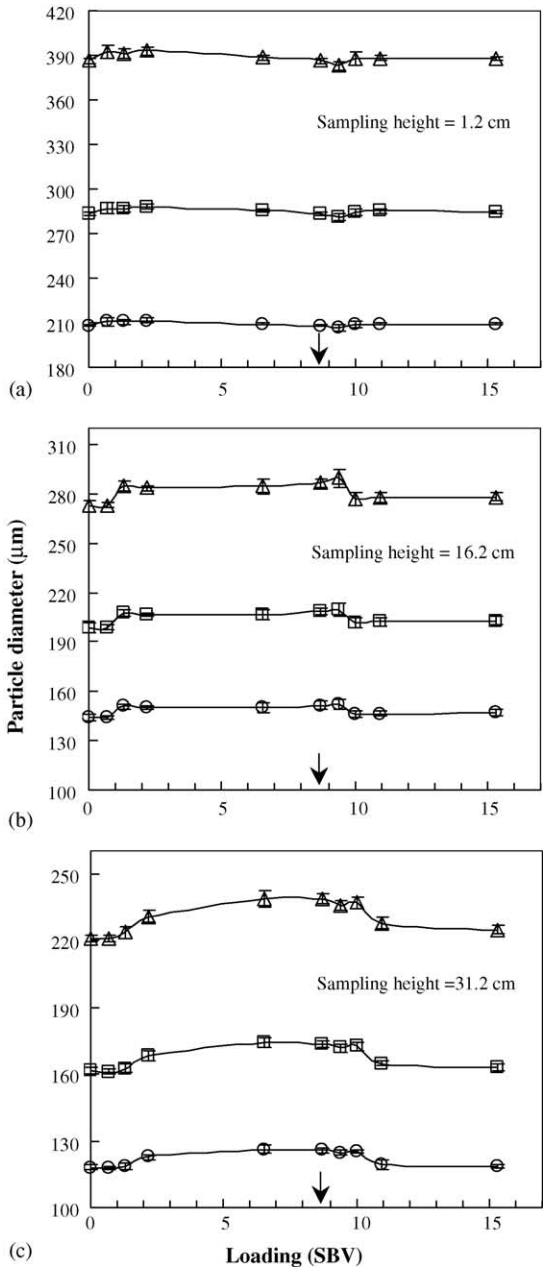

Fig. 6. Variations in particle sizes (◯) d_{10}, (□) d_{50} and (△) d_{90} with mobile phase volume at the three axial heights. Feed solution was changed from deionized water to glycerol solution at 0 min (0 SBV) and then was switched back to deionized water at 40 min (8.74 SBV, indicated by arrow).

another steady state was reached soon after 6 SBV of water (totally 14.74 SBV) was loaded. The way of the variations in bed voidage at the top position (31.2 cm) was similar to that at the middle position, but the initial changes of local voidage with the mobile phases occurred at 2.16 SBV, about 0.86 SBV later than that at the middle position.

The bed voidage distribution results reported by Bruce and Chase [12] and Willoughby et al. [14] were obtained at different experimental conditions with different methods. However, the general range and trend of the variations in the bed voidage measured in this work was reasonably compara-

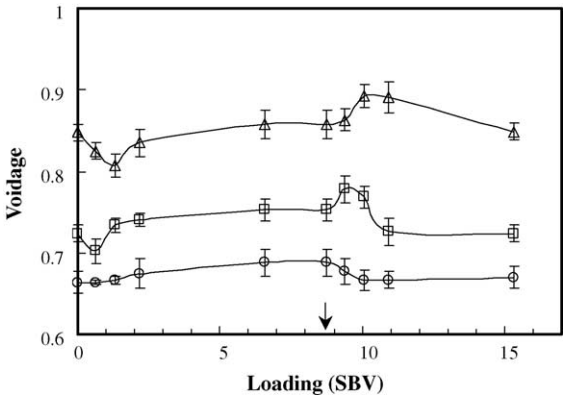

Fig. 7. Bed voidage at the axial heights of (◯) 1.2 cm, (□) 16.2 cm and (△) 31.2 cm as a function of the mobile phase volume. Experimental conditions were the same as in Fig. 6.

ble to the results of Bruce and Chase [12], except for the value in the bottom part (0.50 in the range of 0–10 cm in their work, while 0.66 measured locally herein). Bruce and Chase [12] used the mean residence time method for the measurement. They have pointed out that physically accurate estimates of expanded bed voidage could not be made for the zone between 0 and 10 cm by using the mean residence time method because of the non-uniform flow in this region, and admitted that the measured mean residence time for the bottom zone was shorter than the average behavior in this zone, which led to underestimation of the voidage.

Comparing the results exhibited in Figs. 6 and 7, it can be found that the transient variations in local particle size and voidage distributions initially occurred in the bed bottom and then progressed from bottom to top along the axial direction. These changes at certain sampling positions are considered to be consequent on the flow of a new mobile phase. This is supported by the following estimation of the in-bed flow front using the measured bed voidage values, assuming a plug flow of the mobile phases during the transient processes.

The estimated void volumes for the two zones of 0–16.2 cm and 0–31.2 cm were calculated by using the local voidage values at the two ends of any zone and the porosity of Streamline AC. The void volume below 1.2 cm was estimated by assuming that the bed voidage for this small region was the same as that measured at 1.2 cm. Using the experimental data displayed in Fig. 7, the void volume for the 0–16.2 cm and 0–31.2 cm zones were calculated from the following equation:

$$V_{\text{void}} = V_{\text{zone}}\varphi_{\text{ave}} + \varepsilon_{\text{p}} V_{\text{zone}}(1 - \varphi_{\text{ave}}) \quad (4)$$

where the particle porosity ε_{p} of Streamline AC was taken to be 0.85 [23]. The average bed voidage values for the two zones are approximated by the following calculations.

$$0 - 16.2\,\text{cm zone}: \quad \varphi_{\text{ave}} = \frac{\varphi_1 + \varphi_2}{2} \quad (5)$$

$$0 - 31.2\,\text{cm zone}: \quad \varphi_{\text{ave}} = \frac{\varphi_1 + \varphi_3}{2} \quad (6)$$

All the calculated results are summarized in Table 1.

As shown in Table 1 and Figs. 6 and 7, when the loaded glycerol solution reached 0.65 SBV, the loading volume (40.5 mL) had not surpassed the void volume (76.7 mL) of the lower zone (0–16.2 cm), indicating that the flow front of the glycerol solution was below the height of 16.2 cm. So, the particle size at 1.2 cm increased somewhat because the new mobile phase had passed through this bottom position (Fig. 6a), while the change in particle size distribution at the upper two sampling positions was little (Fig. 6b,c). However, the bed voidages at the upper two positions decreased at this moment (Fig. 7). This is due to the compression effect caused by the upward movement of the lower part particles, resulting from the loading of the high density and viscosity solution. When the glycerol solution loading reached 1.30 SBV, the flow front of glycerol solution had passed over the axial height of 16.2 cm but not yet reached the axial height of 31.2 cm (Table 1). Consequently, the particle size at the

Table 1
Calculated values for the estimation of mobile phase flow front during the transient operation processes

Loading volume (SBV[a])	Loading volume[b] (mL)	Estimated void volume for the 0–16.2 cm zone[c] (mL)	Estimated void volume for the 0–31.2 cm zone[c] (mL)
Phase II (glycerol solution loading)			
0	0	76.8	149.3
0.65	40.5	76.7	149.1
1.30	93.1	76.9	148.9
2.16	162.8	77.0	149.3
6.48	512.7	77.1	149.7
Phase III (deionized water loading)			
0	0	77.1	149.7
0.65	40.5	77.2	149.7
1.30	93.1	77.1	149.9
2.16	162.8	76.8	149.8
6.48	512.7	76.8	149.4

[a] 1 SBV = 81.0 mL.
[b] Excluding the volume of system tubing (12.2 mL).
[c] Including both the bed voidage and particle porosity of Streamline AC.

middle position increased (Fig. 6b) and the voidage there rebounded as well, whereas the particle size at 31.2 cm still remained steadily (Fig. 6c) and the local voidage there continued to decrease. By the continuous loading, the particles at the top position were inevitablly influenced by the solution. When 2.16 SBV was loaded, both the particle size and local voidage at the top position augmented and the increases of the voidage and particle size did not cease until the bed reached a new steady-state.

During the recharge of deionized water at 8.74 SBV, reverse variations in both the particle size distribution (Fig. 6) and local voidage (Fig. 7) occurred in the same sequence from bottom to top as those during the loading process of the glycerol solution. Similar explanation for the transient behavior can be made for the process.

4. Conclusions

To investigate the transient variations of local particle size distribution and bed voidage in the feedstock loading and column washing processes in expanded bed adsorption, 10% (w/w) glycerol solution and deionized water were used as model solutions for the feed solution and washing buffer, respectively. The sampling method for the removal of liquid–solid suspension was employed to measure the changes in local particle size and bed voidage at different axial positions along the column during the transient processes. Variations in the axial particle size distribution during the initial bed expansion were confirmed to progressively develop from the initial uniform distribution in settled bed to an ultimate stable stratification in expanded bed. Changes of local particle size distributions and bed voidage during the conversion in mobile phase viscosity were found to occur in the bed bottom and then progressed from bottom to top along the axial direction. However, the changes of bed voidage at different axial positions were not unidirectional. A prediction for such variations in particle size distributions and bed voidage during the transient operation processes with a dynamic polydisperse model [24] would be a subject of further research.

5. Nomenclature

d_p	particle diameter (m)
g	gravitational constant (9.81 m s^{-2})
n	Richard-Zaki exponent
u_t	terminal velocity of particle (m s^{-1})
u	superficial velocity of mobile phase (m s^{-1})
V_S	settled-bed volume within sampling syringe (mL)
V_{SL}	liquid–solid suspension volume within sampling syringe (mL)
V_{void}	void volume of corresponding zone within expanded bed (mL)
V_{zone}	total volume of a zone within expanded bed (mL)
ε_p	particle porosity of streamline particle
μ	liquid viscosity (Pa s)
ρ	density of mobile phase (kg m^{-3})
ρ_p	particle density (kg m^{-3})
φ	expanded-bed voidage
φ_S	settled-bed voidage of sample
φ_{ave}	average bed voidage of certain zone within bed
φ_1	local bed voidage at axial height of 1.2 cm or bed bottom
φ_2	local bed voidage at axial height of 16.2 cm
φ_3	local bed voidage at axial height of 31.2 cm

Acknowledgements

This work was financially supported by the Natural Science Foundation of China (grant No. 20025617). We thank G.-Y. Sun and X.-Y. Zhao for their assistance in the sampling work.

References

[1] H.A. Chase, Trends Biotechnol. 12 (1994) 296.
[2] F.B. Anspach, D. Curbelo, R. Hartmann, G. Garke, W.-D. Deckwer, J. Chromatogr. A 865 (1999) 129.
[3] E.S.D. Santos, R. Guirardello, T.T. Franco, J. Chromatogr. A 944 (2002) 217.
[4] R.H. Clemmitt, H.A. Chase, Biotechnol. Bioeng. 82 (2003) 506.
[5] H.M. Fernández-Lahore, R. Kleef, M.-R. Kula, J. Thömmes, Biotechnol. Bioeng. 64 (1999) 484.
[6] H.M. Fernández-Lahore, S. Geilenkirchen, K. Boldt, A. Nagel, M.-R. Kula, J. Thömmes, J. Chromatogr. A 873 (2000) 195.
[7] J. Feuser, M. Halfar, D. Lütkemeyer, N. Ameskamp, M.-R. Kula, Pro. Biochem. 34 (1999) 159.
[8] D.-Q. Lin, M.-R. Kula, A. Liten, J. Thömmes, Biotechnol. Bioeng. 81 (2003) 21.
[9] D.-Q. Lin, P.J. Brixius, J.J. Hubbuch, J. Thömmes, M.-R. Kula, Biotechnol. Bioeng. 83 (2003) 149.
[10] I. Theodossiou, O.R.T. Thomas, J. Chromatogr. A 8971 (2002) 73.
[11] A. Karau, C. Benken, J. Thömmes, M.-R. Kula, Biotechnol. Bioeng. 55 (1997) 54.
[12] L.J. Bruce, H.A. Chase, Chem. Eng. Sci. 56 (2001) 3149.
[13] Y. Bai, C.E. Glatz, Biotechnol. Bioeng. 81 (2003) 856.
[14] N.A. Willoughby, R. Hjorth, N.J. Titchener-Hooker, Biotechnol. Bioeng. 69 (2000) 648.
[15] X.D. Tong, Y. Sun, J. Chromatogr. A 977 (2002) 173.
[16] J. Yun, S.-J. Yao, D.-Q. Lin, M.-H. Lu, W.-T. Zhao, Chem. Eng. Sci. 59 (2004) 449.
[17] Amersham Pharmacia Biotech, Expanded Bed Adsorption—Principles and Methods, Handbook, Pharmacia Biotech, Uppsala, 1999.
[18] J.F. Richardson, W.N. Zaki, Trans. Int. Chem. Eng. 32 (1954) 35.
[19] L. De Luca, D. Hellenbroich, N.J. Titchener-Hooker, H.A. Chase, Bioseparation 4 (1994) 311.
[20] L.J. Bruce, H.A. Chase, Chem. Eng. Sci. 57 (2002) 3085.
[21] X. Hu, Chem. Eng. Technol. 25 (2002) 911.
[22] P.L. Slis, T. Willemse, H. Kramers, Appl. Sci. Res. 8 (1959) 209.
[23] B. Xue, Y. Sun, Chem. Eng. Sci. 58 (2003) 1531.
[24] B. Xue, X.D. Tong, Y. Sun, AIChE. J. 49 (2003) 2150.